Radiocarbon, Vol 65, Nr 6, 2023, p 1280–1298 DOI:10.1017/RDC.2023.126
© The Author(s), 2024. Published by Cambridge University Press on behalf of University of Arizona. This is an Open Access article, distributed under the terms of the Creative Commons Attribution licence (http://creativecommons.org/licenses/by/4.0/), which permits unrestricted re-use, distribution and reproduction, provided the original article is properly cited.

CHRONOLOGICAL MODELING ON A CALIBRATION PLATEAU: IMPLICATIONS FOR THE EMERGENCE OF AGRICULTURE IN THE DUTCH WETLANDS

Merita Dreshaj[1,2*] • Daan Raemaekers[1] • Michael Dee[3]

[1]University of Groningen, Groningen Institute of Archaeology, Groningen, the Netherlands
[2]Centre for Isotope Research, Groningen, the Netherlands
[3]University of Groningen, Centre for Isotope Research, Groningen, the Netherlands

ABSTRACT. Short-duration archeological sites situated entirely within plateaus in the radiocarbon calibration curve pose unique challenges for our understanding of past processes at regional and global scales. This paper aims to overcome these limitations by leveraging the specific characteristics of two depositional contexts, the Early Neolithic Swifterbant Culture sites S3 and S4, located in the Dutch wetlands. These sites are of exceptional significance as they provide the earliest conclusive evidence of crop cultivation and animal husbandry outside the expansion of Linearbandkeramik (LBK) farmers in north-western Europe. Here, we present a customized approach that combines radiocarbon dating and Bayesian modeling, predicated on vertical sequences of short-lived plant remains. Our innovative approach enables us to determine, at a fine scale, the temporal position and duration of the prominent archeological contexts at S3 and S4, and explore the chronological relationship between the two sites. Through our analysis, we propose a new chronology for the onset of Neolithization in the Dutch wetlands.

KEYWORDS: Bayesian modeling, calibration plateau, Dutch wetlands, radiocarbon dating, Swifterbant.

INTRODUCTION

The surge in the use of Bayesian chronological modeling, in combination with advances in radiocarbon measurement and an improved calibration curve (Reimer et al. 2020) has enabled "generational precision" to be achieved for some archeological chronologies (Whittle and Bayliss 2007; Bronk Ramsey 2009; Dee et al. 2013; Kuitems et al. 2020). Notwithstanding these advancements, calibration plateaux continue to pose challenges to precision by generating wide date ranges, irrespective of the uncertainties of the associated raw measurements (Taylor et al. 1996). Short duration sites situated entirely within a calibration plateau and lacking the possibility of wiggle matching represent a specific challenge for high-precision dating. In these cases, the availability of reliable stratigraphic sequences of radiocarbon dates becomes even more crucial (Buck et al. 1991; Hamilton et al. 2015).

This case study focuses on the Swifterbant Culture sites S3 and S4 in the province of Flevoland, the Netherlands (Figure 1). The Swifterbant Culture holds significant importance in the discourse on the Neolithization process in the plains of northwestern Europe, with archeological sites spanning across the Netherlands, the Scheldt valley in Belgium, and Lower Saxony in Germany. This situates them just north-west of the "loess belt," an area settled by the first European farming communities, the Linearbandkeramik culture (hereafter "LBK") that utilized the fertile topsoil of the wind-blown loess sediments stretching across a substantial portion of central and southeast Europe (Whittle 1996; Bakels 2009).

Despite proximity and interaction with these farmers, the Swifterbant communities persisted as hunter-gatherers for centuries. They eventually introduced subsistence novelties, including pottery use, animal husbandry and crop cultivation, all the while heavily relying on hunting and gathering practices (Raemaekers et al. 2021).

*Corresponding author. Email: m.dreshaj@rug.nl

https://doi.org/10.1017/RDC.2023.126 Published online by Cambridge University Press

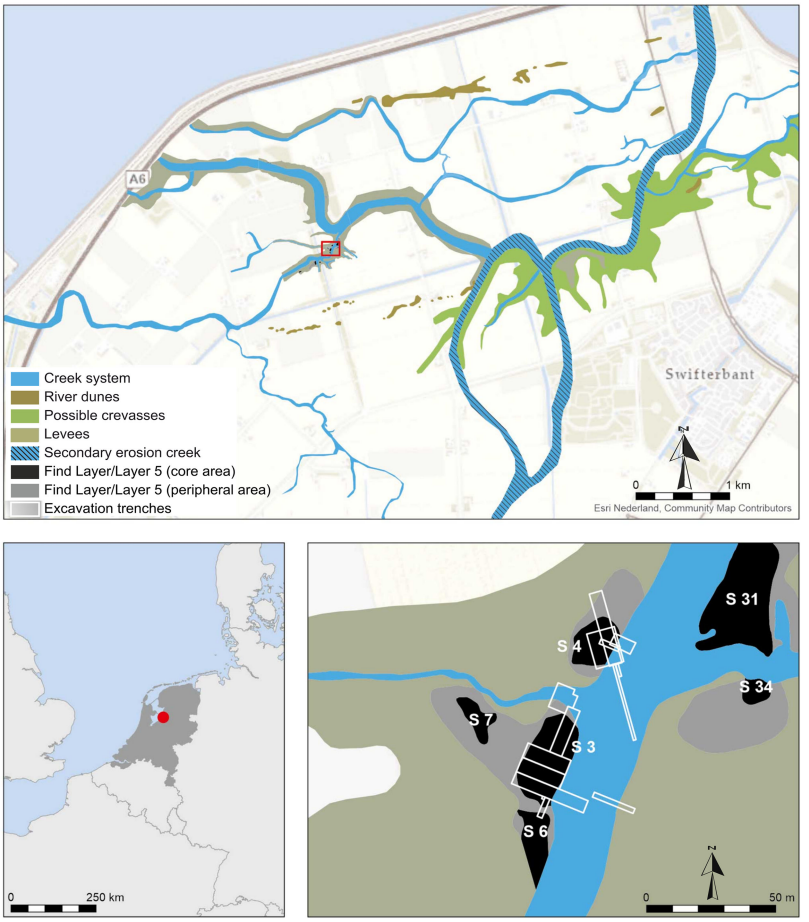

Figure 1 Maps showing the location of S3 and S4 sites (upper part) and the Netherlands in relation to Europe, with marked position of the sites (bottom left). Insert (bottom right): Detailed view on S3 and S4 with the outline of excavation trenches and the environment at the time (4300–4000 BCE).

The prevailing interpretation presupposes a gradual and prolonged transition to agriculture, potentially predating neighboring regions such as the British Isles and southern Scandinavia. This positions Swifterbant as a pivotal milestone in the transition to agriculture outside of the LBK zone in north-western Europe (Zvelebil and Rowley-Conwy 1986; Rowley-Conwy et al. 2020; Sørensen 2020; Raemaekers et al. 2021).

However, the precise timing and duration of this process has been the subject of intense debate (Raemaekers et al. 2021), largely due to the limited availability of comprehensive multi-proxy and chronological research on keystone sites (Dreshaj et al. 2022). Notably, the Swifterbant sites of S3 and S4 hold exceptional significance as they provide the oldest conclusive evidence of cultivated fields and early animal management and are remarkably well preserved (Cappers and Raemaekers 2008; Huisman et al. 2009; Huisman and Raemaekers 2014; Schepers and Woltinge 2020; Brusgaard et al. forthcoming).

https://doi.org/10.1017/RDC.2023.126 Published online by Cambridge University Press

However, the chronology of these sites falls entirely within the calibration plateau spanning the period 4300–4000 BCE. As a result, individual calibrated dates lack the resolution needed to avoid coarse interpretation of the activities associated with these important subsistence changes (Dreshaj et al. 2022).

Our ultimate objective was to overcome these limitations and to improve the chronological resolution of these processes. To accomplish this, we employed a multifaceted approach. Given the absence of clear-cut stratigraphy but little to no post-depositional disturbance (Huisman et al. 2009), we chose to sample charred short-lived plant remains from the vertical columns of excavation spits for radiocarbon dating. This approach allowed us to define the chronological order of the sampled material, which offered crucial prior information for the Bayesian modeling. In combination with carefully vetted legacy data, robust models were constructed. Based on the modeling outcomes, we propose an improved timeframe for the commencement of agriculture in the Dutch wetlands.

Description of the Sites

The Swifterbant sites S3 and S4 are located in Oostelijk Flevoland, a polder in the Netherlands that was reclaimed from the floor of lake IJsselmeer in the 1950s. Like much of the country, during the Holocene this area was influenced by sea-level rise, causing the extension of peat and clay deposits in tidal gullies (Schepers and Woltinge 2020). Consequently, it transformed into a freshwater, low-energy environment characterized by minimal transportation of large sediment particles and the accumulation of fine-grained sediments, such as those found in lagoons, estuaries, and deltas (Ente 1976; Dalrymple et al. 1992; Schepers and Woltinge 2020). Within this setting, small creeks and river branches formed, creating an environment where very fine sediments were continuously deposited along the banks (Huisman et al. 2009; Huisman and Raemaekers 2014; Schepers and Woltinge 2020). It was in this context that a series of dwellings and cultivated fields associated with prehistoric Swifterbant culture were discovered. Among these sites, S3 and S4 (Figure 1) have been particularly well-studied (van der Waals 1977; Raemaekers and Roever 2020).

Excavations at S3 and S4 revealed evidence of intense anthropogenic presence. Finds varied from large amounts of carbonized plant and bone remains, pottery, flints, and features such as charcoal marks, posts and postholes, remains of surface hearths, as well as burials (van der Waals 1977; Schepers and Woltinge 2020). In fact, due to striking similarities in stratigraphy and archaeological evidence as well as the proximity of both sites, excavators proposed that the sites likely started as one and were later divided by a gully (Schepers and Woltinge 2020).

At both sites, these archeological features and materials were associated exclusively with a prominent thick dark layer known as the "Find Layer" at S3 and "Layer 5" at S4. Both layers commence at a similar elevation of approximately 6.3–6.5 meters below sea level, exhibiting a gentle slope (van der Waals 1977; Schepers and Woltinge 2020). At S3, this layer was approximately 100 cm thick, while at S4, it was about half this. Both layers were interpreted as a succession of organic material depositions, primarily burnt reed rushes (mats), recognizable as discontinuous ~1.0–1.5 cm thick micro-laminations. As this presented challenges in archeological field recording, systematic excavation was conducted in 5 cm spits (van der Waals 1977; Schepers and Woltinge 2020). At S4, the excavators estimated that there was a sequence of ~35 layers, which might correspond to a similar number of years if deposition occurred annually. A comparable observation was made at the S3 site, which was expected to span ~80–100 years. Recording by spits was applied only within the context of the Find Layer/

https://doi.org/10.1017/RDC.2023.126 Published online by Cambridge University Press

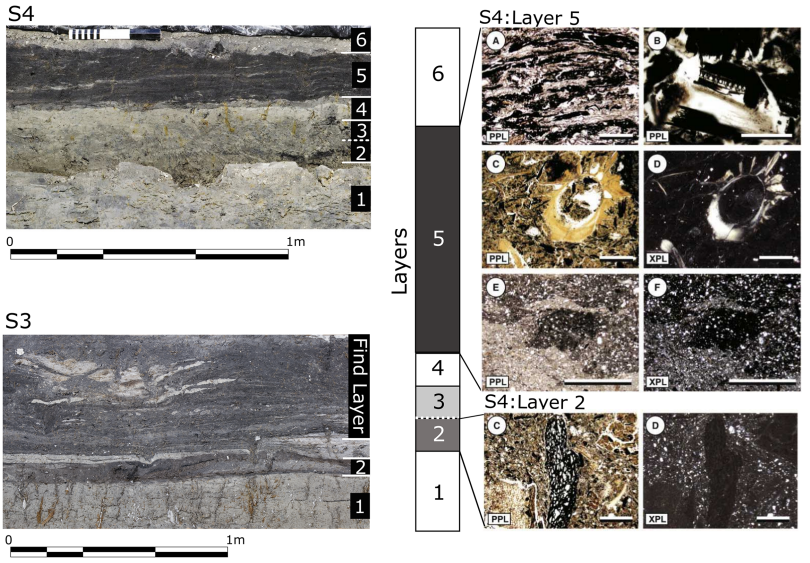

Figure 2 Overview of layers associated in S3 and S4. Left: photographs of profile sections of S4 and S3, with marked layers, adapted from Huisman and Raemaekers (2014: Fig. 4) and Schepers and Woltinge (2020: Fig. 2.3). N.B. Division of layers is a combination of the two publication: Layer 3 and 4 both correspond to layer III, and Layer 5 and 6 correspond to Layer IV and V in Huisman et al. (2009), respectively. Right: Scheme of layers and thin sections with micromorphological features associated with Layer 5 and Layer 2 at S4. Layer 5: micro-laminations (A), organic matter (B, E, F) and coprolites (C, D). Layer 2: carbonized plant fragments in vertical position, indicating tillage (C, D). Adapted from Huisman et al. (2009: Fig. 5, p. 192, Fig. 6, p. 195, Fig. 7, p. 197). For more details on this study, refer to Huisman et al. (2009).

Layer 5 because the remainder of the stratigraphical units seemed sterile (van der Waals 1977; Geuverink 2020; Schepers and Woltinge 2020).

A comprehensive understanding of the taphonomy, occupational timeline, and function of the Swifterbant S4 site was pursued through a micromorphological study. It revealed the exceptional preservation and micro-laminations of Layer 5 (Layer IV in Huisman et al. 2009) (Figure 2), which had been largely undisturbed by post-depositional processes. Indeed, the absence of indicators for trampling led to the proposition that S4 served as a refuse area or midden, rather than a dwelling (Huisman et al. 2009).

Furthermore, the analysis unveiled evidence of anthropogenic activities extending beyond Layer 5, into the layers above and below that were previously assumed sterile. These activities were primarily manifested as evidence of tillage practices associated with *in situ* farming, observed in the underlying Layer 2 as well as Layer 6, which overlies Layer 5 (Huisman et al. 2009; Huisman and Raemaekers 2014; Figure 2). An archeobotanical study further supported these findings, noting the increased prevalence of naked barley in older spits (5–9) and the significant influx of other plant species linked to daily settlement activities in younger spits (1–4) (Schepers and Bottema-MacGillavry 2020). This evidence strengthens the argument that S4 underwent several changes in its function: from a farming area (Layer 2) to a refuse site (Layer 5) and eventually reverted to its initial role (Layer 6) (Huisman et al. 2009; Huisman and Raemaekers 2014; Schepers and Woltinge 2020).

https://doi.org/10.1017/RDC.2023.126 Published online by Cambridge University Press

Table 1 List of stratified legacy dates from S4 and S3.

Sample no.	Site	Layer/ m NAP	material	Date (BP)	±	Publication
GrA-38188	S4	Layer 2	Reed	5230	40	Schepers and Woltinge 2020.
GrA-38189	S4	Layer 2	Reed	5340	45	Schepers and Woltinge 2020.
GrN 7042	S3	6,10 m	Charcoal	5295	40	Van der Waals 1977.
GrN 7044	S3	6,05 m	Wood	5310	50	Van der Waals 1977.
GrN 7043	S3	5,75 m	Charred wood	5375	40	Van der Waals 1977.

The absence of micromorphological research at S3 leaves us without specific details regarding post-depositional disturbance and the nature of anthropogenic activities at this site. However, excavators at S4, when reviewing the field documentation of S3, retroactively concluded the depositional pattern at S3 exhibits similarities to S4 (van der Waals 1977; Schepers and Woltinge 2020:20–22).

Regarding subsistence practices, which play a crucial role in understanding the significance of these sites within the Neolithization debate, multiple lines of evidence support the presence of animal husbandry. Cattle comprise the majority of the faunal assemblage at both sites, followed by domesticated pigs and various wild animals such as red deer and beaver (Clason and Brinkhuizen 1978; Zeiler 1997; Kranenburg and Prummel 2020; Brusgaard et al. forthcoming). Recent zooarcheological and stable isotope studies on the faunal assemblage of S3 and S4 have shed further light on dietary management and potential transhumance practices related to cattle (Brusgaard et al. Forthcoming). These findings align with the archeobotanical identification of grassland plant communities, which is indicative of grazing activities (Schepers 2014). Taken together, the combination of these results provides compelling evidence of early animal management in the Dutch wetlands (Brusgaard et al. forthcoming).

Legacy Radiocarbon Dates

The legacy datasets from Swifterbant sites S3 and S4 include 23 radiocarbon dates obtained from various materials such as short-lived plant remains, ruminant collagen, wood, charcoal, and human collagen (refer to Supplementary Information (hereafter "SI") Table 1) (van der Waals 1977; Lanting and Plicht 2000; Devriendt 2013; Schepers and Woltinge 2020). All of these dates fall within the calibration plateau (4300–4000 BCE) and yield wide ranges, except for three exceptional cases. Two older dates, measured on charred food remains on pottery and collagen from human bone, likely exhibit a reservoir effect (UtC-1046, GrA-6488, respectively), although this claim is difficult to substantiate in the absence of $\delta^{15}N$ values. Additionally, one short-lived sample from the upper part of Layer 5 at S4 returns a significantly younger age. Considering its position and context within the site (SI: Table 1), it is possible that this sample represents an intrusive element from a later phase of site utilization, as observed in the exploitation history of the area (Huisman et al. 2009; Peeters et al. 2021).

An ever-present challenge lies in the lack of precise contextual allocation for most of the legacy dates within the Find Layer/Layer 5 itself. Only three dates from the Find Layer at S3 have documented superposition (hereafter "stratified legacy dates") (Table 1). The remainder of dates have not reached a degree of reliability necessary for our study. In addition, two dates

https://doi.org/10.1017/RDC.2023.126 Published online by Cambridge University Press

from S4 were sampled from the underlying Layer 2 (van der Waals 1977; Huisman et al. 2009; Schepers and Woltinge 2020), offering an additional constraint for chronological modeling. Despite these caveats, the exceptional preservation and minimal post-depositional disturbance observed in the refuse layer at both sites provide a unique opportunity for conducting high-resolution chronological research.

METHODS

New Radiocarbon Analyses

Our study aimed to utilize the exceptionally undisturbed nature of the context in order to overcome the lack of detailed stratigraphy and combat the calibration plateau. Hence, we selected samples from various depths along the spits of each vertical column, enabling us to establish clearly defined chronological sequences. Furthermore, to ensure the highest quality radiocarbon measurements, we prioritized short-lived, clearly anthropogenic materials that were abundant and had well-documented contextual information. Specifically, we collected 31 charred seeds (*Hordeum vulgare* or naked barley) from six vertical columns (three per site) within the Find Layer at S3 and Layer 5 at S4 (Figure 3). Our sampling was limited to these layers because material from other contexts contained insufficient supporting information.

Prior to the chemical pretreatment process, all samples underwent species-level identification and were photographed using a Leica m-125c microscope coupled with a Mc 190HD camera (Figure 4, SI: Fig 1_SI, Fig 2_SI, Fig 3_SI, Fig 4_SI).

The routine chemical pretreatment for charred plant remains at the Centre for Isotope Research at the University of Groningen is outlined in Dee et al. (2020). Briefly, all samples were decalcified in acid ($HCl_{(aq)}$, 4% w/vol, 80°C, 30 min). Next, all samples were rinsed with decarbonized and demineralized water (DW) three times, followed by a base ($NaOH_{(aq)}$ 1%, w/vol, 80°C, 30 min) and another triplicate rinse with demineralized water (3×). To avoid the incorporation of $CO_{2(g)}$ from the atmosphere, another step of acid ($HCl_{(aq)}$, 4% w/vol, 80°C, 30 min), followed by a final set of three rinses with DW was applied. All samples were air-dried. Aliquots 3–4 mg in size of the reduced carbon extracts were subsequently weighed into $Sn_{(s)}$ capsules and combusted in an Elemental Analyzer (EA, Elemental Vario Isotope Cube) coupled to an Isotope Ratio Mass Spectrometer (IRMS, IsoPrime 100) and an automated cryogenic system which traps the $CO_{2(g)}$ into sealable glass vessels. This allowed for the determination of $\delta^{13}C$. The $CO_{2(g)}$ was then graphitized over a $Fe_{(s)}$ catalyst in a stoichiometric excess of $H_{2(g)}$ employing an in-house built graphitization system. Finally, the graphite was pressed into $Al_{(S)}$ cathodes and transferred to the MICADAS mass spectrometer (Ionplus AG 200kV) for radioisotope analysis. For pretreatment quality assurance, each batch included a known-age sample, in this case charred seeds from Bronze Age Jericho (see Dee et al. 2020), and to corroborate the stable isotope analyses, IAEA caffeine ($\delta^{13}C = -38.2‰$) and oxalic acid ($\delta^{13}C = -17.60‰$) were concomitantly measured as standards.

Bayesian Models

We used the OxCal program in this study (Bronk Ramsey 2009) and the IntCal20 calibration curve (Reimer et al. 2020). OxCal functions are denoted with capital letters throughout.

Our modeling strategy follows our sampling rationale. Specifically, we were able to translate each column of radiocarbon dates into Sequences in OxCal. A simple bounded Phase

https://doi.org/10.1017/RDC.2023.126 Published online by Cambridge University Press

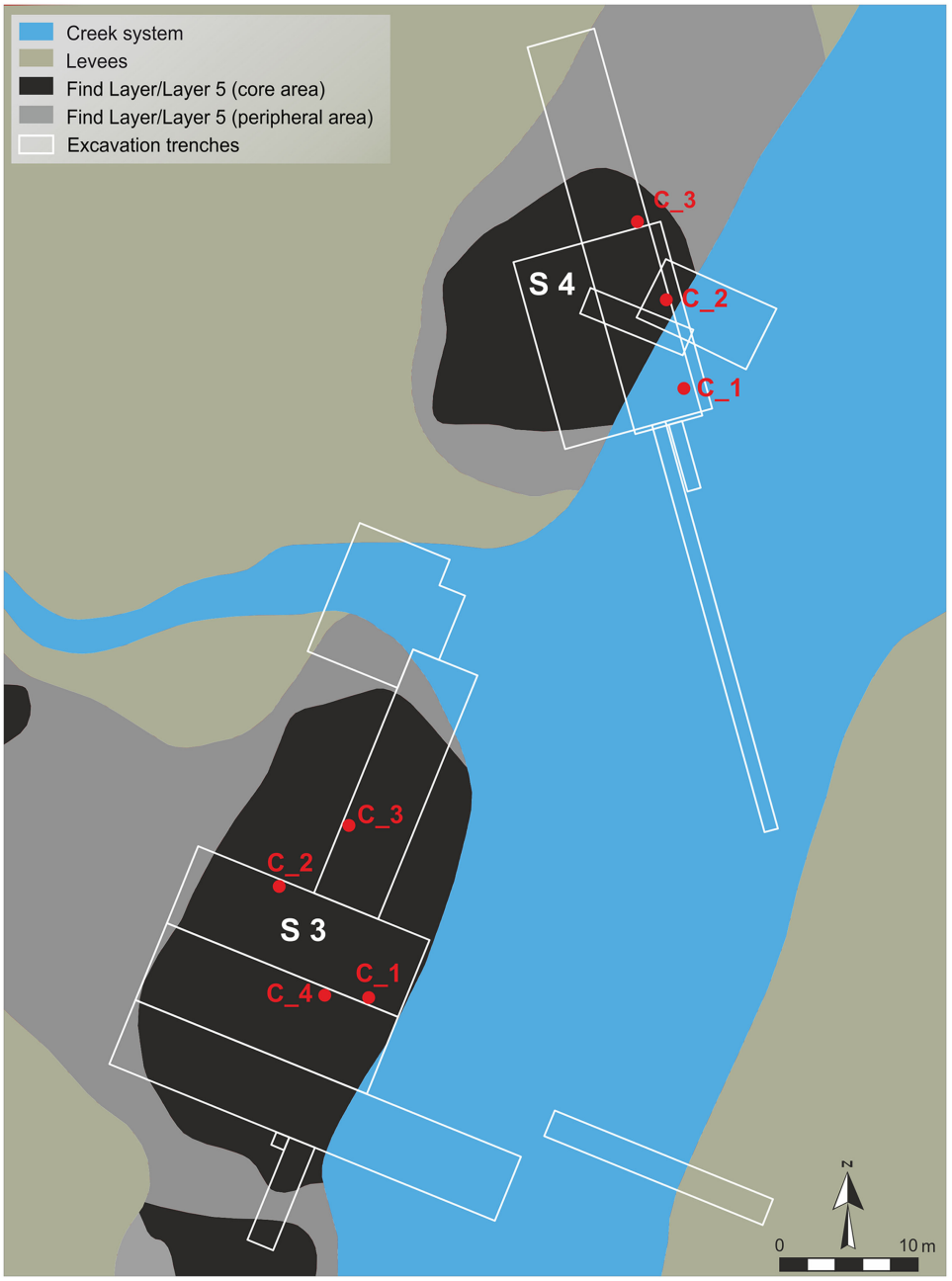

Figure 3 Position of sampled columns of new radiocarbon dates (C1-3) and a column of legacy dates (C4) at S3 and S4. After Devriendt 2013. Fig. 2.7, adjusted.

encompassed all these Sequences per site (Figure 5). We applied the General Outlier model with an outlier probability of 0.05 and utilized the Charcoal Plus function for the legacy dates obtained from charcoal and wood samples (Dee and Bronk Ramsey 2014) (see SI for codes). To analyze the duration of the contexts, we employed the Sum and Interval functions. The

https://doi.org/10.1017/RDC.2023.126 Published online by Cambridge University Press

Figure 4 Photographs of charred *Hordeum vulgare* seeds (Leica m-125c coupled to Mc 190HD camera) sampled for radiocarbon dating: GrM-27307 from S3 and GrM-28294 from S4.

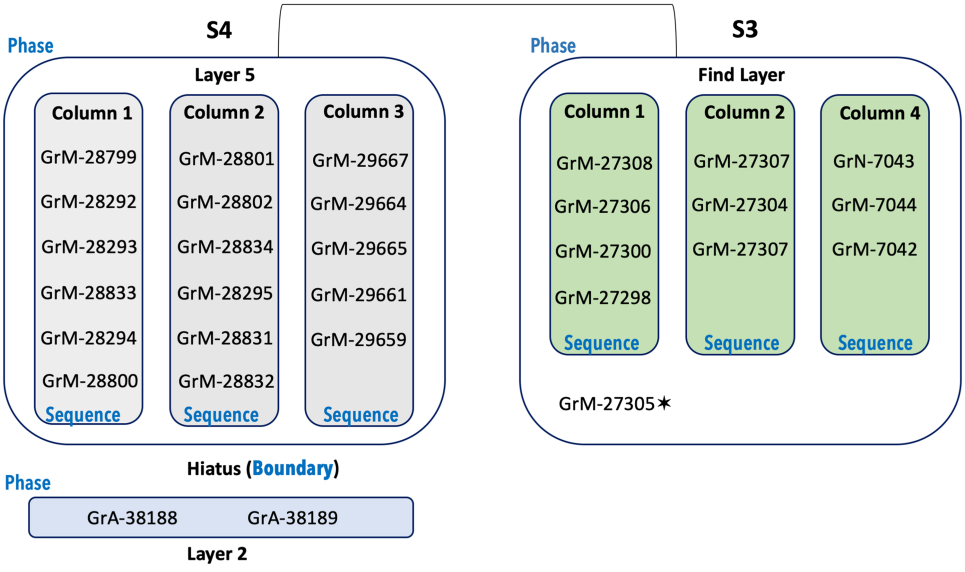

Figure 5 Scheme of the modelling strategy of new radiocarbon dates, with added selected legacy dates from Layer 2 and Column 4 from Find Layer at S3 (Model 2). Date GrM-27305* is the only successful new radiocarbon date from Column 3.

former sums posterior probability densities of all dates within the designated grouping, whereas the latter calculates intervals between events in a Sequence, specifically between the Boundaries of a Sequence. This gives an estimate of the probable number of years for the occurrence of an event (Bronk Ramsey 2009).

Further, we explored the hypothesis that all 6 columns, 3 at each site, were simultaneously deposited since they were traversed in the same archeological layers, but in different areas of the sites. That is, we investigated the possibility that the evidence for occupation in each of the columns began and ended at the same time. To this end, we extracted the prior probabilities for

https://doi.org/10.1017/RDC.2023.126 Published online by Cambridge University Press

the Start and End Boundaries of each Sequence, and Combined them to form even further refined estimates, albeit heavily dependent on this assumption of synchronicity.

We built two main models: Model 1, which only incorporated the new dates, and Model 2, which also included five legacy dates with known contextual superimposition.

Alternative models were prepared to investigate the reproducibility and robustness of the results. These included models without Outlier Analysis and models without stratigraphical assignment (grouping dates into a simple bounded Phase). Furthermore, legacy data that lacked any contextual definition were also combined with the stratified dates to examine their impact on the model outcomes. Additionally, simulations were prepared to assess how the incremental inclusion of additional dates would affect the resolution of the models (for codes, see SI). All models ran to completion.

RESULTS AND DISCUSSION

In total, 25 samples yielded sufficient carbon for radiocarbon analysis. All known-age samples, treated in concert with the archeological material, returned results within acceptable ranges, confirming the quality of analyzed batches. As expected, all samples produced probability distributions on the calibration plateau, and remarkably similar uncalibrated ages (Table 2).

Model 1: New Radiocarbon Dates Only

The output of Model 1 (Figure 6) exhibited significantly narrowed down individual dates. However, at both S3 and S4 sites, the 95% probability ranges split into two distinct modes, which can be ascribed to minor fluctuations in the calibration plateau (Figure 7).

Notably, at S4, the modeled probabilities strongly favored the older mode. Most of the output sits between 4250 and 4160 BCE, with only a fraction of probability between 4100 and 4060 BCE. Indeed, ~80% range of modeled probabilities of each date within Sequences at S4 are between 4240 and 4160 BCE. The output of the Interval function suggests a very short-term, likely single generational occupation, and has a median value of 30 years.

The Start and End Boundaries of each Sequence at S4 were almost identical (Figure 6), and combining the posterior probabilities of all three columns constrained the output entirely to the older mode, even at 95% probability. As a result, taking all the aforementioned assumptions to be valid, we were able to get very precise Start and End Boundaries for Layer 5 at the S4 site (Figure 6). In summary, we propose that the most plausible time range for this context is 4240–4160 BCE.

For the S3 dataset, the 95% ranges of the posterior probability densities span most of the calibration plateau, but they coalesce between ~4180 and 4030 BCE at 68% probability. The relative imprecision of these ranges may be attributed to either too few new or the greater time-depth of the site, which makes it more challenging to anchor individual dates within the calibration plateau.

However, our sensitivity tests, which involved incrementally adding simulated dates to investigate the impact of a larger radiocarbon dataset, showed no significant differences in the model's outcome (see SI). Therefore, we conclude that additional radiocarbon dates within the Find Layer may not significantly contribute to the chronological resolution of this site.

https://doi.org/10.1017/RDC.2023.126 Published online by Cambridge University Press

https://doi.org/10.1017/RDC.2023.126 Published online by Cambridge University Press

Table 2 Radiocarbon measurements on charred plant remains (*Hordeum vulgare* seeds). Sample pretreatment and analysis were carried out at the Centre for Isotope Research, Groningen.

Lab ID	Sample no.	Site	Context	$F^{14}C$	± (1σ)	^{14}C age (yr BP)	± (1σ)	%C	δ ^{13}C (‰, v. PDB)	± (1σ)
GrM-29664	S4_1299	S4	Layer 5, Spit 2	0.5156	0.0012	5321	27	56.1	–24.89	0.15
GrM-29665	S4_2299	S4	Layer 5, Spit 3	0.5152	0.0012	5327	29	53.7	–24.37	0.15
GrM-29661	S4_3299	S4	Layer 5, Spit 4	0.5149	0.0012	5332	27	55.4	–25.88	0.15
GrM-29659	S4_4299	S4	Layer 5, Spit 5	0.5166	0.0012	5306	27	55.8	–22.45	0.15
GrM-29667	S4_288	S4	Layer 5, Spit 1	0.5165	0.0012	5307	27	60.2	–24.52	0.15
GrM-28799	S4_409	S4	Layer 5, Spit 1	0.5139	0.0017	5348	27	58.9	–25.06	0.15
GrM-28292	S4_1409	S4	Layer 5, Spit 2	0.5139	0.0018	5348	27	49.8	–23.23	0.15
GrM-28293	S4_2409	S4	Layer 5, Spit 3	0.5138	0.0017	5349	27	55.6	–23.34	0.15
GrM-28833	S4_3409	S4	Layer 5, Spit 4	0.5149	0.0020	5330	30	60.5	–25.04	0.15
GrM-28294	S4_4409	S4	Layer 5, Spit 5	0.5159	0.0015	5317	24	59.5	–24.89	0.15
GrM-28800	S4_6409	S4	Layer 5, Spit 7	0.5118	0.0017	5380	27	69.3	–25.69	0.15
GrM-28801	S4_538	S4	Layer 5, spit 1	0.5114	0.0017	5387	27	57.9	–25.32	0.15
GrM-28802	S4_4559	S4	Layer 5, spit 5	0.5127	0.0017	5366	27	61.7	–23.76	0.15
GrM-28295	S4_6559	S4	Layer 5, spit 7	0.5145	0.0011	5338	16	63.4	–24.09	0.15
GrM-28831	S4_7589	S4	Layer 5, spit 8	0.5129	0.0020	5365	30	64.4	–24.48	0.15
GrM-28832	S4_9588	S4	Layer 5, spit 10	0.5139	0.0021	5350	30	56.5	–25.32	0.15
GrM-27308	14-XI-F	S3	Level F (1)	0.5204	0.0017	5247	26	52.6	–24.18	0.15
GrM-27306	14-XI-G	S3	Level G (2)	0.5188	0.0018	5272	28	50.5	–25.06	0.15
GrM-27300	15-XII-H	S3	Level H (3)	0.5226	0.0017	5213	26	60.8	–25.42	0.15
GrM-27298	14-XII-K	S3	Level K (5)	0.5170	0.0016	5300	26	52.3	–23.46	0.15
GrM-27307	23-XV-F	S3	Level F (1)	0.5212	0.0018	5235	28	51.2	–24.53	0.15
GrM-27310	24-XVI-I	S3	Level I (4)	0.5151	0.0016	5329	26	50.1	–27.40	0.15
GrM-27304	24-XVI-K	S3	Level K (5)	0.5153	0.0016	5326	26	51.8	–24.62	0.15
GrM-27305	20-XXII-G	S3	Level G (2)	0.5172	0.0016	5297	26	57.1	–24.35	0.15

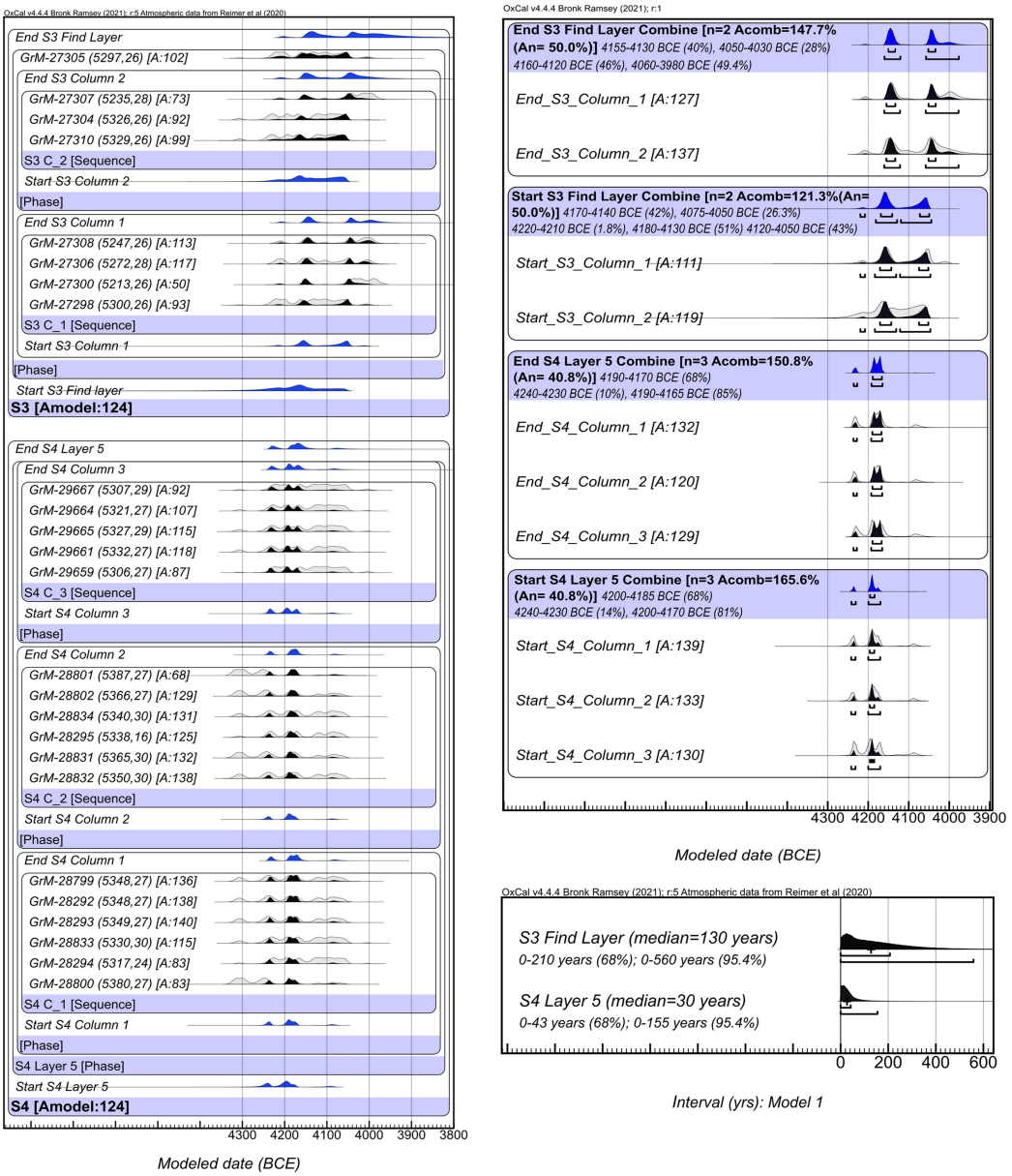

Figure 6 Model 1. (Left) The posterior probability densities of individual dates. Modeled dates are marked in black, unmodeled in light gray and Boundaries in blue. OxCal functions are denoted in "[ ]" for clarity. (Upper right) Estimated Boundaries of S4 and S3 sites, after Combining Prior data on Boundaries from each column. (Bottom right) Estimated Intervals for radiocarbon dated layers at S3 and S4. For codes, refer the SI.

The output of the Interval function at S3 suggests a longer occupation than S4, with a median of approximately 130 years (Figure 6). This supports the hypothesis that S3 has a greater time depth than S4, potentially indicating that it was a multigenerational site. The greater width of the Find Layer, the presence of younger pottery types, and a higher number of (micro)layers at S3 further reinforce this interpretation (van der Waals 1977; Raemaekers 2015).

https://doi.org/10.1017/RDC.2023.126 Published online by Cambridge University Press

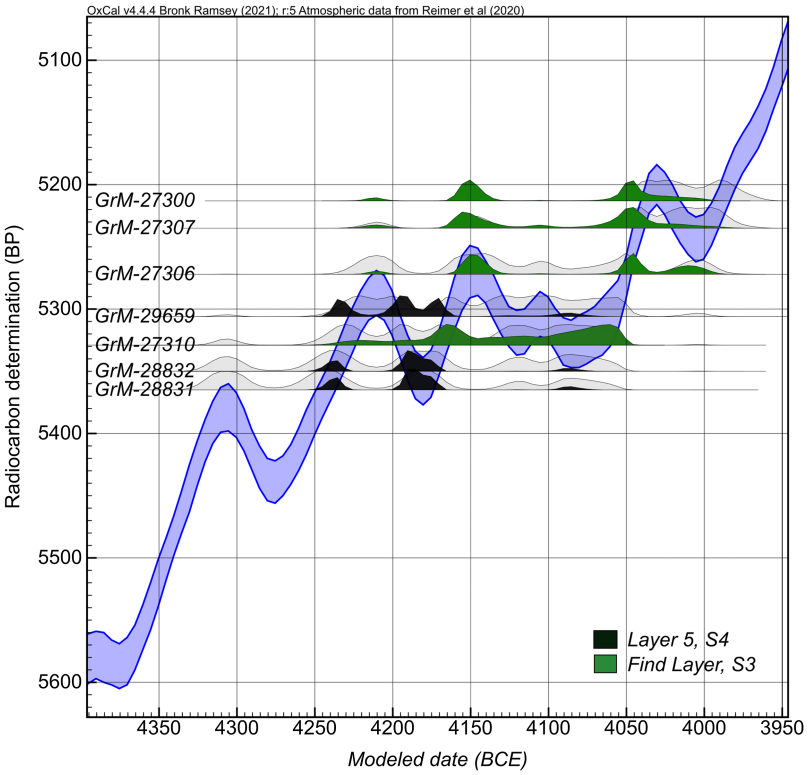

Figure 7 Model 1. The posterior probability densities of selected dates on a calibration curve; more specifically—calibration plateau 4300–4000 BCE. The individual dates are color coded to reflect their contextual allocation.

In contrast to S4, the Boundaries of each Sequence at S3 exhibit a continued bimodal distribution. However, all Sequences appear to be simultaneous (Figure 6).

In our sensitivity tests, where we omitted the contextual prior information, and simply grouped all the dates into a bounded Phase, the outputs of the Start and End Boundaries and the Interval results were comparable to Model 1 (see SI). Such repetitively consistent outputs act to confirm the reliability of our main models.

Model 2: New and Selected Legacy Radiocarbon Dates

In Model 2 (Figure 8, 9), the inclusion of legacy dates in the S3 site significantly increased the sample size by introducing an additional column (Sequence). However, this addition had minimal impact on the modeled dates compared to Model 1, except for a slight reduction in the Interval median to 100 years.

In comparison, the S4 dates in Model 2 exhibit a notable change in the output due to the inclusion of two dates from Layer 2 underlying the hiatus and Layer 5. This constraint narrows down the older mode of posterior probabilities of dates for this layer to a time range between ~4200 and 4160 BCE. This range is in accordance with the Interval, which reflects a short-term, likely single-generational, anthropogenic presence (Figure 8). As a result of this constraint, any

https://doi.org/10.1017/RDC.2023.126 Published online by Cambridge University Press

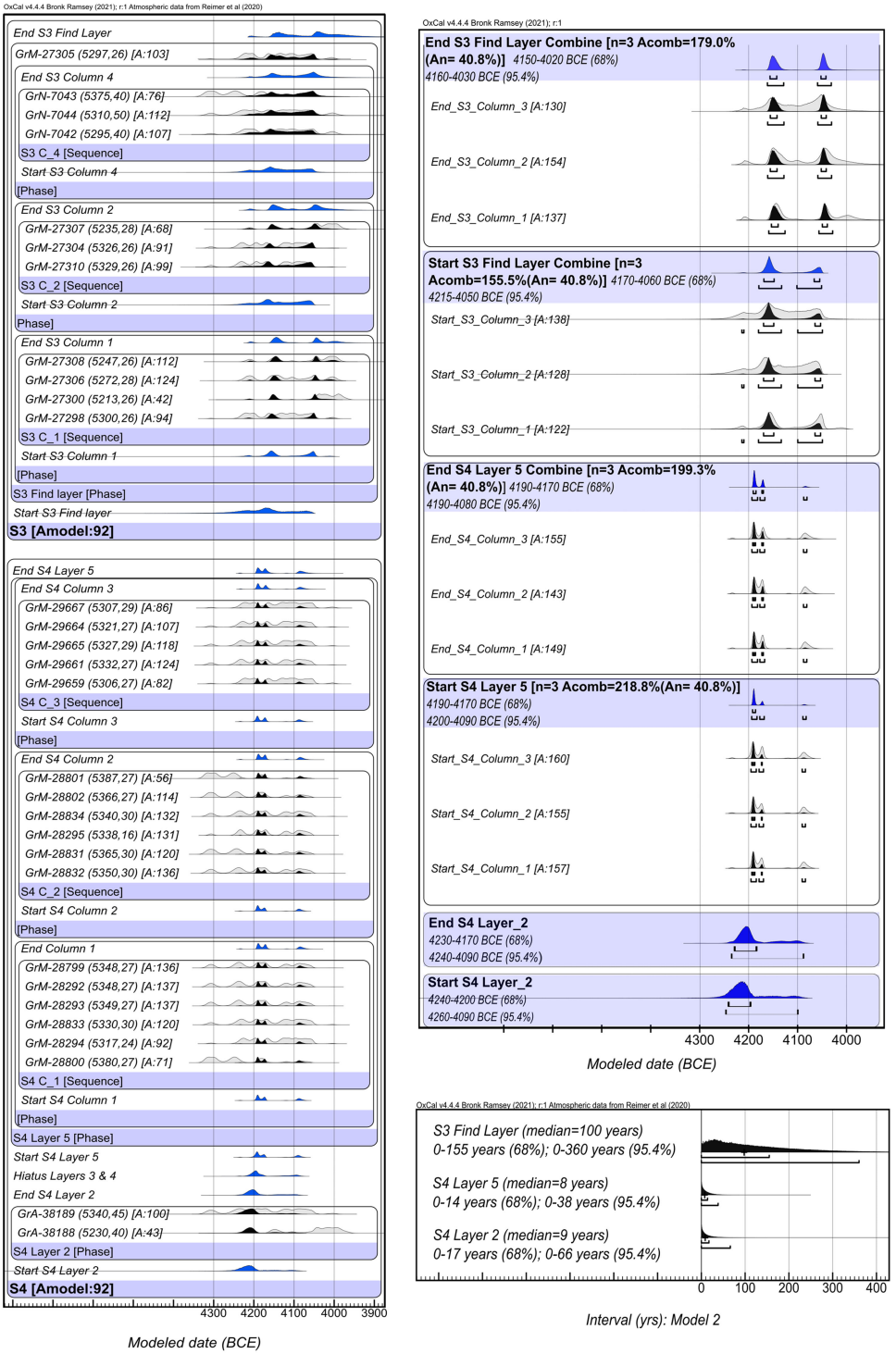

Figure 8 (Left) The probability densities from Model 2. Modeled dates are marked in black, unmodeled in light gray and Boundaries in blue. OxCal functions are denoted in "[ ]" for clarity. (Upper right) Modeled Start and End Boundaries of vertical columns from S3 and S4 sites, including Combined Boundaries. (Bottom right) Estimated Intervals for radiocarbon dated layers at S3 and S4. For codes, refer to the SI.

https://doi.org/10.1017/RDC.2023.126 Published online by Cambridge University Press

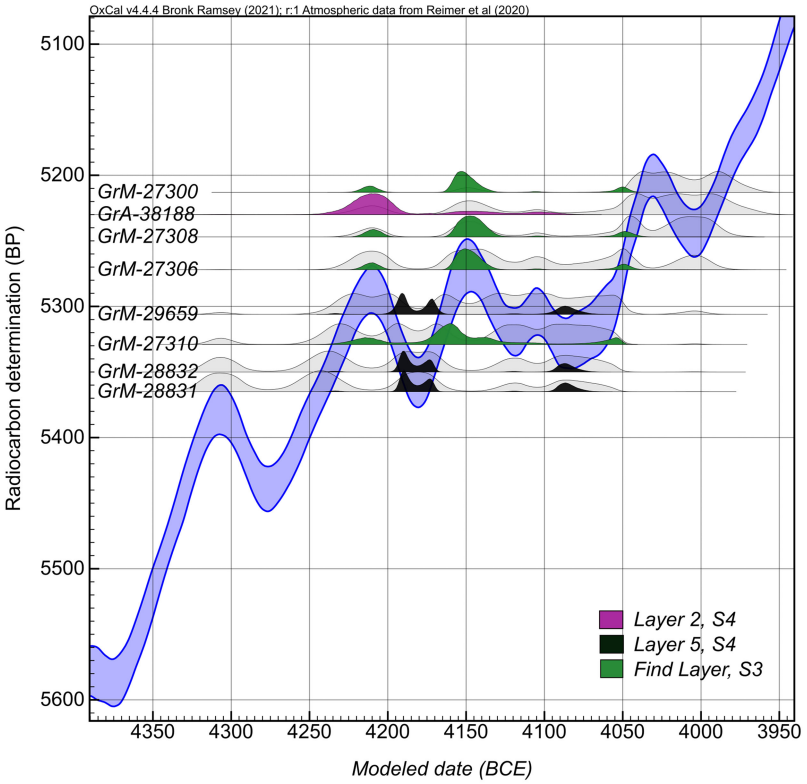

Figure 9 Model 2. The posterior probability densities of selected dates on a calibration curve; more specifically—calibration plateau 4300–4000 BCE. The individual dates are color coded to reflect their contextual allocation.

probability extending older than 4200 BCE was excluded, leading to a slightly stronger preference for the younger mode compared to Model 1. This is likely due to the absence of an additional constraint *above* Layer 5. However, the older mode still contains the majority of the remaining probability, which is in accordance with the results from Model 1.

In Model 2, we were able to calculate a more precise date range of Layer 2, associated with the oldest evidence of farming practices in the area (Huisman et al. 2009; Huisman and Raemaekers 2014). Modelled probabilities of both dates from this context fall between 4240 and 4190 BCE at 68% (1σ) range (Figure 8), with a minor portion of probability extending until 4100 BCE. The probability output for Start and End Boundaries follow the same pattern, with 68% (1σ) ranges 4240–4200 BCE and 4230–4170 BCE, respectively. The output of the Interval function for this layer indicates this event was of a punctuated nature, with median values of only ~9 years. Similarly, the output of the Interval function for Layer 5 is significantly shorter than Model 1, returning a similar duration to Layer 2 (Figure 8).

Much like Model 1, the comparison of the Boundaries of each Sequence within these sites confirms their simultaneity (Figure 8). Additionally, when comparing the Boundaries of each Sequence using the Combine function, S3 shows no significant difference from Model 1. However, in the case of S4, the bimodal distribution for the Combined Start and End Boundary

https://doi.org/10.1017/RDC.2023.126 Published online by Cambridge University Press

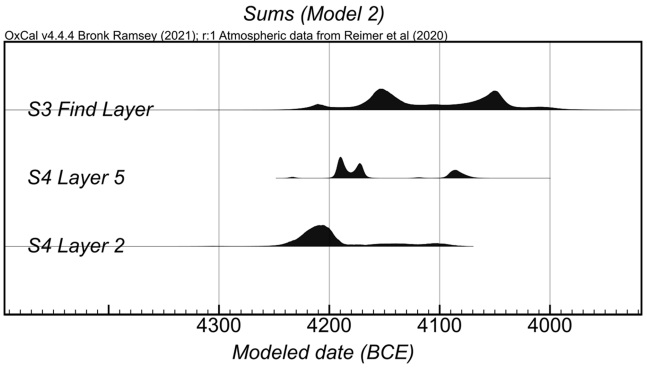

Figure 10 Sums of probability distributions for layers at S4 and S3.

remains. Approximately 5% of the posterior probability lies between 4100 and 4080 BCE, while the majority (90%) of the distribution lies between 4200 and 4170 BCE. This distribution aligns with the pattern of a slight increase in preference towards the younger mode. Nonetheless, as the vast majority of the posterior probability remains within the range of 4200 and 4170 BCE, we propose that the chronology of S4 falls within these ranges.

Notably, the test models without any enforced Sequencing (simple bounded Phases for each layer) showed no significant difference in the outcomes observed (SI).

Inter-Site Chronological Comparison

The comparison of the Start and End Boundaries of the S3 and S4 sites (using the Combine function) indicates that the initiation and cessation of anthropogenic activity in Layer 5 and underlying Layer 2 at S4 were likely not simultaneous to the Find layer at S3 (Figure 8). Assuming our hypotheses are accurate, we propose the following sequence of events at S4: the agricultural field in Layer 2 was likely established first, followed by a relatively brief hiatus (Layer 3/4) in keeping with the archeological evidence, and subsequently succeeded by the refuse activity represented in Layer 5. The anthropogenic activities associated with both layers at S4 appear to have been short-term, possibly spanning a single generation or less.

Determining the extent of overlap between Layer 5 at S4 and Find Layer at S3 is challenging due to the presence of multimodal posterior distribution densities. There is an overlap in the modeled distribution densities of Sums (Figure 10), and the Boundaries at S3 cover a significant portion of the calibration plateau (Figure 8). The greater occupational time at S3 may contribute to the wider posterior densities observed.

Adding the constraint of further radiocarbon dates below Layer 5, as was the case with the two dates available from Layer 2, in Model 2, demonstrated the potential of additional sampling from layers outside of the Find layer (e.g. tillage marks, see Huisman et al. 2009; Huisman and Raemaekers 2014). This can create a "sandwich effect" constraining the outputs and would have the potential to greatly enhance the chronological resolution of the S3 site. Future excavation or coring campaigns should consider implementing this strategy to further improve chronological precision.

https://doi.org/10.1017/RDC.2023.126 Published online by Cambridge University Press

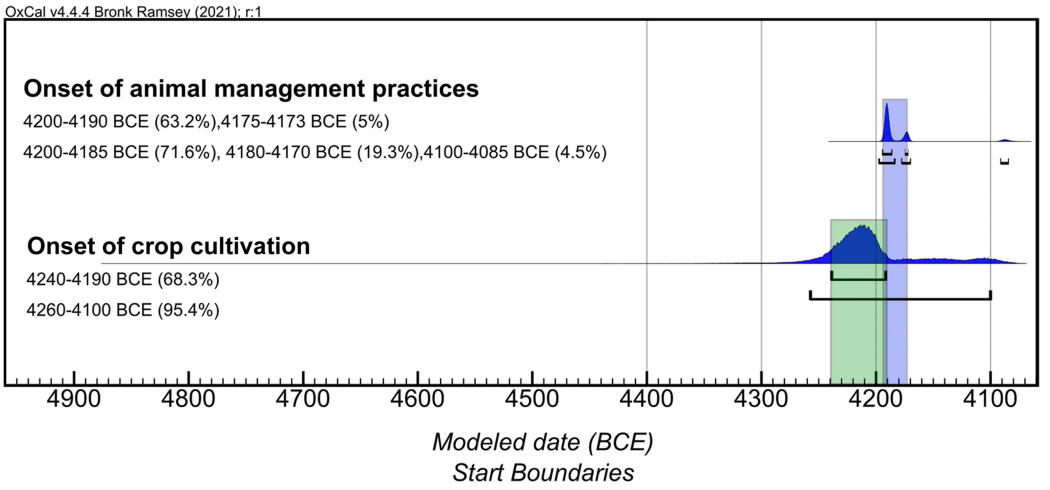

Figure 11 Estimated probability ranges for the onset of new subsistence practices in the Dutch wetlands. The former is the Start Boundary for Layer 2 (Phase) and the latter, Combined Start Boundary for Layer 5, based on radiocarbon measurements of spit 1 in all three vertical columns (Sequences), Model 2. Colored are 68% ranges where the bulk of probability lies.

Nevertheless, what is clear from our study is that anthropogenic presence at S4 commenced before S3 and had a significantly shorter duration which is in excellent accordance with the archeological evidence and observations made by the excavators, as discussed above (van der Waals 1977; Schepers and Woltinge 2020).

Through our analysis, we not only achieved significant improvements in dating precision and the chronostratigraphies of these important sites but also determined the onset of the earliest known farming activity and animal management in this area (Figure 11). Based on our findings (Model 2), we propose that the emergence of cereal cultivation in the Dutch wetlands took place between 4240 and 4190 BCE (68.3% probability, or 4260–4100 BCE, 95%, Start Boundary Layer 2). This is followed by the emergence of animal management practices, as evidenced in Layer 5, S4, estimated to occur between 4200 and 4170 BCE (90.5% probability, Start Boundary Layer 5).

CONCLUSION

Obtaining higher chronological resolution for short-duration sites located entirely on the calibration plateau, without the possibility of wiggle matching, presents several challenges. These challenges are further compounded by the absence of archeological layer stratification, ambiguous documentation of legacy data, and radiocarbon dates affected by inbuilt age.

In this paper, we presented a case study of the S3 and S4 Swifterbant sites, situated in the Dutch wetlands, which are considered pivotal for understanding the earliest stages of crop cultivation and animal management in the region. To overcome the lack of a well-defined sequence of archeological layers, we employed a novel approach. We radiocarbon dated unambiguously anthropogenic short-lived organic material from vertical sequences across the stratigraphic profiles and conducted Bayesian analysis. Through this method, we were able to refine

https://doi.org/10.1017/RDC.2023.126 Published online by Cambridge University Press

the individual dates and investigate the temporal synchronicity between these two sites. The robustness of our models was confirmed through sensitivity tests.

Our analysis suggests the following timeframe of subsistence changes in the Dutch wetlands, with the majority of the probability falling within these ranges: the onset of cereal cultivation is estimated to take place between 4240 and 4190 BCE (68.3% probability), followed by the emergence of animal management practice between 4200 and 4170 BCE (90.5% probability).

The results of this study reveal an intriguing observation. The Swifterbant communities within the Dutch wetlands adopted crop cultivation and animal management practices within the span of a single generation, while still maintaining a nomadic and seasonal way of life. These results challenge the previously held belief of a gradual long introduction of agriculture in the area, suggesting instead a more punctuated process.

When we compare these results to evidence from neighboring regions outside the expansion of the Linearbandkeramik culture, such as the British Isles, Ireland, and South Scandinavia, agriculture seems to have been established in the Dutch wetlands at least two centuries earlier than in the neighboring regions. This raises interesting questions about the relationships between communities in these areas and the local dynamics surrounding the introduction of new subsistence practices, challenging the broad supra-regional narratives.

ACKNOWLEDGMENTS

The authors extend their gratitude to Arnoud Maurer and Dr. Rene Cappers for their valuable archeobotanical expertise and assistance with sample selection. Additionally, the insightful discussions with Dr. Hans Huisman and Dr. Mans Schepers were pivotal in shaping the conceptual framework of this paper.

This study is part of the project "The Emergence of Domesticated Animals in the Netherlands," funded by the Dutch Research Council (NWO) (grant number 406.18.HW.026.) The funders had no role in study design, data collection and analysis, the decision to publish, or the preparation of the manuscript.

SUPPLEMENTARY MATERIAL

To view supplementary material for this article, please visit https://doi.org/10.1017/RDC.2023.126.

REFERENCES

Bakels C. 2009. The beginning: 5300 BC–4900 BC. In: The Western European Loess Belt. Dordrecht: Springer. p. 29–54. https://doi.org/10.1007/978-1-4020-9840-6_3

Bronk Ramsey C. 2009. Bayesian analysis of radiocarbon dates. Radiocarbon 51(1). https://doi.org/10.1017/S0033822200033865

Brusgaard NØ, Kooistra J, Schepers M, Dee M, Raemaekers D, Çakirlar C. Accepted and Forthcoming. Early animal management in northern Europe: new multi-proxy evidence from Swifterbant, the Netherlands. Antiquity.

Buck CE, Kenworthy JB, Litton CD, Smith AFM. 1991. Combining archaeological and radiocarbon information: a Bayesian approach to calibration. Antiquity 65(249). https://doi.org/10.1017/S0003598X00080534

Cappers RTJ, Raemaekers DCM. 2008. Cereal cultivation at Swifterbant? Neolithic Wetland Farming on the North European Plain. Current Anthropology 49(3):385–402. https://doi.org/10.1086/588494

Clason AT, Brinkhuizen DC. 1978. Swifterbant, mammals, birds, fishes. A preliminary report.

https://doi.org/10.1017/RDC.2023.126 Published online by Cambridge University Press

(Swifterbant contribution 8). Helinium, 18: 69–82.

Dalrymple RW, Zaitlin BA, Boyd R. 1992. Estuarine facies models; conceptual basis and stratigraphic implications. Journal of Sedimentary Research 62(6):1130–1146. https://doi.org/10.1306/D4267A69-2B26-11D7-8648000102C1865D

Dee M, Ramsey CB. 2014. High-precision Bayesian modeling of samples susceptible to inbuilt age. Radiocarbon 56(1):83–94. https://doi.org/10.2458/56.16685

Dee M, Wengrow D, Shortland A, Stevenson A, Brock F, Girdland Flink L, Bronk Ramsey C. 2013. An absolute chronology for early Egypt using radiocarbon dating and Bayesian statistical modelling. Proceedings of the Royal Society A: Mathematical, Physical and Engineering Sciences 469(2159):20130395. https://doi.org/10.1098/rspa.2013.0395

Dee MW, Palstra SWL, Aerts-Bijma AT, Bleeker MO, Bruijn S de, Ghebru F, Jansen HG, Kuitems M, Paul D, Richie RR, Spriensma JJ, Scifo A, Zonneveld D van, Verstappen-Dumoulin BMAA, Wietzes-Land P, Meijer HAJ. 2020. Radiocarbon dating at Groningen: new and updated chemical pretreatment procedures. Radiocarbon 62(1):63–74. https://doi.org/10.1017/RDC.2019.101

Devriendt IIJALM. 2013. Swifterbant stones: The Neolithic stone and flint industry at Swifterbant (the Netherlands) [thesis]. University of Groningen.

Dreshaj M, Dee M, Peeters H, Raemaekers D. 2022. Blind dates: Exploring uncertainty in the radiocarbon evidence on the emergence of animal husbandry in the Dutch wetlands. Journal of Archaeological Science: Reports 45. https://doi.org/10.1016/j.jasrep.2022.103589

Ente PJ. 1976. The Geology of the northern part of Flevoland in relation to the human occupation in the Atlantic time. Swifterbant Contribution 2. Helinium 16(1):15–35.

Geuverink J. 2020. Features and spatial analysis. In Swifterbant S4 (The Netherlands). Occupation and exploitation of a Neolithic levee site (c. 4300-4000 cal.BC). Barkhuis. p. 98–106.

Hamilton WD, Haselgrove C, Gosden C. 2015. The impact of Bayesian chronologies on the British Iron Age. World Archaeology 47(4):642–660. https://doi.org/10.1080/00438243.2015.1053976

Huisman DJ, Jongmans AG, Raemaekers DCM. 2009. Investigating Neolithic land use in Swifterbant (NL) using micromorphological techniques. CATENA 78(3):185–197. https://doi.org/10.1016/j.catena.2009.03.006

Huisman DJ, Raemaekers DCM. 2014. Systematic cultivation of the Swifterbant wetlands (The Netherlands). Evidence from Neolithic tillage marks (c. 4300–4000 cal. BC). Journal of Archaeological Science 49:572–584. https://doi.org/10.1016/j.jas.2014.05.018

Kranenburg H, Prummel W. 2020. The use of domestic and wild animals on S4. In: Raemaekers DCM and de Roever JP (eds.), Swifterbant S4. Occupation and exploitation of a Neolithic levee site (Groningen Archaeological Series). Groningen. Barkhuis. p. 76–94. https://doi.org/10.2307/j.ctv13nb6ns

Kuitems M, Panin A, Scifo A, Arzhantseva I, Kononov Y, Doeve P, Neocleous A, Dee M. 2020. Radiocarbon-based approach capable of subannual precision resolves the origins of the site of PorBajin. Proceedings of the National Academy of Sciences of the United States of America 117(25):14038–14041. https://doi.org/10.1073/pnas.1921301117

Lanting JN, Plicht J van der. 2000. De 14C-chronologie van de Nederlandse pre- en protohistorie, III: Neolithicum. Palaeohistoria 1–110. https://ugp.rug.nl/Palaeohistoria/article/view/24984

Peeters JHM, Asscher T, Kooistra LI, Kubiak-Martens L, Zeiler J. 2021. Exploiting a changing landscape: Subsistence, habitation and skills. In: Resurfacing the submerged past. Prehistoric archaeology and landscapes of the Flevoland Polders, the Netherlands. p. 67–128. https://www.sidestone.com/books/resurfacing-the-submerged-past

Raemaekers D. 2015. Rethinking Swifterbant S3 ceramic variability: Searching for the transition to the Funnel Beaker culture before 4000 calBC. The Dabki Site in Pomerania and the Neolithisation of the North European Lowlands (c. 5000-3000 CalBC). p. 321–334.

Raemaekers D, Demirci Ö, Kamjan S, Talebi T, Schepers M, Huisman H, Peeters H, Çakirlar C. 2021. Timing and Pace of Neolithisation in the Dutch Wetlands (c. 5000–3500 cal. BC). Open Archaeology, 7(1): 658–670. https://doi.org/10.1515/opar-2020-0157

Raemaekers D, Roever JP, editors. 2020. Swifterbant S4 (the Netherlands). Occupation and exploitation of a Neolithic levee site (c. 4300-4000 cal. BC). Barkhuis.

Reimer PJ, Austin WEN, Bard E, Bayliss A, Blackwell PG, Ramsey CB, Butzin M, Cheng H, Edwards RL, Friedrich M, Grootes PM, Guilderson TP, Hajdas I, Heaton TJ, Hogg AG, Hughen KA, Kromer B, Manning SW, Muscheler R, Talamo S. 2020. The IntCal20 Northern Hemisphere radiocarbon age calibration curve (0–55 cal kBP). Radiocarbon 62(4):725–757. https://doi.org/10.1017/RDC.2020.41

Rowley-Conwy P, Gron KJ, Bishop RR, Dunne J, Evershed R, Longford C, Schulting R, Treasure E. 2020. The earliest farming in Britain: Towards a new synthesis. In: Gron KJ, Sorensen L, Rowley-Conwy P, editors. Farmers at the frontier: a pan European perspective. Oxbow Books. p. 401–424. https://www.oxbowbooks.com/oxbow/farmers-at-the-frontier.html

https://doi.org/10.1017/RDC.2023.126 Published online by Cambridge University Press

Schepers M. 2014. Reconstructing vegetation diversity in coastal landscapes. Barkhuis. https://doi.org/10.2307/j.ctt2250tg8

Schepers M, Bottema-MacGillavry N. 2020. The vegetation and exploitation of plant resources. In: Raemaekers DCM, de Roever JP, editors. Swifterbant S4 (the Netherlands): occupation and exploitation of a Neolithic levee site (c. 4300-4000 cal. BC) (Vol. 36, pp. 51–75). Barkhuis. https://doi.org/10.2307/j.ctv13nb6ns

Schepers M, Woltinge I. 2020. Landscape development and stratigraphy. In: Raemaekers D, de Roever P, editors. Swifterbant S4 (p. 15–23). Barkhuis Publishing.

Sørensen L. 2020. Biased data or hard facts?: Interpretations of the earliest evidence of agrarian activity in southern Scandinavia from 6000 to 4000 cal BC in a theoretical discourse on random down-the-line exchanges and structured migrations. In: Sørensen L, Gron KJ, Rowley-Conwy P, editors. Farmers at the frontier. Oxbow Books. p. 289–316. https://doi.org/10.2307/j.ctv13gvh1g.18

Taylor RE, Stuiver M, Reimer PJ. 1996. Development and extension of the calibration of the radiocarbon time scale: Archaeological applications. Quaternary Science Reviews 15(7):655–668. https://doi.org/10.1016/0277-3791(96)00024-8

van der Waals JD. 1977. Excavation at the natural levee site S2 S3/5 and S4. Swifterbant Contribution 6:17(3–27).

Whittle A. 1996. Europe in the Neolithic. The creation of new worlds. Cambridge University Press.

Whittle A, Bayliss A. 2007. The times of their lives: from chronological precision to kinds of history and change. Cambridge Archaeological Journal 17(1): 21–28. https://doi.org/10.1017/S0959774307000030

Zeiler JT. 1997. Hunting, fowling and stock-breeding at neolithic sites in the western and central Netherlands [thesis]. University of Groningen.

Zvelebil M, Rowley-Conwy P. 1986. Foragers and farmers in Atlantic Europe. In: Hunters in transition. Mesolithic societies of temperate Eurasia and their transition to farming. Cambridge University Press. p. 67–93.

https://doi.org/10.1017/RDC.2023.126 Published online by Cambridge University Press